Virologica Sinica 38 (2023) 448–458

Contents lists available at ScienceDirect

Virologica Sinica

journal homepage: www.keaipublishing.com/en/journals/virologica-sinica
www.virosin.org

Research Article

Spastin is required for human immunodeficiency virus-1 efficient replication through cooperation with the endosomal sorting complex required for transport (ESCRT) protein

Wenyuan Shen [a,b,c,1], Chang Liu [a,1], Yue Hu [a,d], Qian Ding [a], Jiabin Feng [a], Zhou Liu [a], Xiaohong Kong [a,*]

[a] Laboratory of Medical Molecular Virology, School of Medicine, Nankai University, Tianjin, 300071, China
[b] Department of Spine Surgery, The Second Hospital of Shandong University, Cheeloo College of Medicine, Shandong University, Jinan, 250033, China
[c] International Science and Technology Cooperation Base of Spinal Cord Injury, Tianjin Key Laboratory of Spine and Spinal Cord Injury, Tianjin Medical University General Hospital, Tianjin, 300052, China
[d] Department of Infectious Diseases, Tianjin Second People's Hospital, Tianjin, 300192, China

ARTICLE INFO

Keywords:
HIV-1 replication
Spastin
Gag production
Lysosomal degradation
Endosomal sorting complex required for transport (ESCRT)

ABSTRACT

Human immunodeficiency virus-1 (HIV-1) encodes simply 15 proteins and thus depends on multiple host cellular factors for virus reproduction. Spastin, a microtubule severing protein, is an identified HIV-1 dependency factor, but the mechanism regulating HIV-1 is unclear. Here, the study showed that knockdown of spastin inhibited the production of the intracellular HIV-1 Gag protein and new virions through enhancing Gag lysosomal degradation. Further investigation showed that increased sodium tolerance 1 (IST1), the subunit of endosomal sorting complex required for transport (ESCRT), could interact with the MIT domain of spastin to regulate the intracellular Gag production. In summary, spastin is required for HIV-1 replication, while spastin-IST1 interaction facilitates virus production by regulating HIV-1 Gag intracellular trafficking and degradation. Spastin may serve as new target for HIV-1 prophylactic and therapy.

1. Introduction

Human immunodeficiency virus type 1 (HIV-1), the pathogen responsible for acquired immunodeficiency syndrome (AIDS), is a complex retrovirus that encodes structural proteins Gag, Pol, and Env, along with six additional accessory proteins Vif, Vpu, Vpr, Tat, Nef, and Rev (Frankel and Young, 1998). Even though multiple host cellular proteins restrict HIV-1 infection, HIV-1 exploits a variety of host cell proteins to facilitate viral infection (Ghimire et al., 2018; Tian et al., 2022). For example, cytoplasmic junction-associated protein 2 (CLASP2) promotes HIV-1 infection by using its C-terminal domain to bind incoming HIV-1 particles and stabilize host cell microtubules (Mitra et al., 2020). The cellular eukaryotic elongation factor 1 (eEF1) complex associates with the HIV-1 reverse transcription complex (RTC) and the association is important for late steps of reverse transcription (Li et al., 2015). P-TEFb complex binds the viral Tat protein and activates the RNA polymerase II transcription of the integrated provirus (Chiang et al., 2012; Ghimire et al., 2018). Tsg101 is required for HIV-1 budding by linking the p6 domain of HIV-1 Gag to vacuolar protein sorting machinery (Garrus et al., 2001; Yang et al., 2018). Histone chaperone CAF-1 promotes HIV-1 latency by leading the formation of phase-separated suppressive nuclear bodies (Ma et al., 2021). So, cellular proteins are essential for HIV-1 replication and may serve as viable new targets for prophylactic and therapy.

A previous study performed a large-scale small interfering RNA screen to identify required host factors for HIV-1 replication and spastin is one of the HIV-1 dependency factors (Brass et al., 2008). Spastin is a microtubule-severing protein that breaks long microtubules into shorter fragments (Kuo et al., 2019; Liu et al., 2022; Roll-Mecak and Vale, 2008). It regulates microtubule dynamics in microtubule-dependent cellular processes, including axonal transport, neurite outgrowth, endosomal recycling, cytokinesis, and endoplasmic reticulum shaping (Li et al., 2021; Lopes et al., 2020; Lumb et al., 2012; Riano et al., 2009; Vajente et al., 2019). Spastin has two main isoforms, one produces a full-length

* Corresponding author.
E-mail address: kongxh@nankai.edu.cn (X. Kong).
[1] Wenyuan Shen and Chang Liu contributed equally to this work.

https://doi.org/10.1016/j.virs.2023.05.006
Received 2 August 2022; Accepted 8 May 2023
Available online 11 May 2023

isoform called M1 and the other produces a slightly shorter isoform called M87. M1 is exclusively present in rat and human adult spinal cord, whereas the M87 is ubiquitously present and more abundant than M1 (Deluca et al., 2004; Solowska and Baas, 2015). M87 had more active microtubule-severing activity than M1 in rat and human spastin constructs transfected cells (Solowska and Baas, 2015; Solowska et al., 2017).

There are three main domains in M1 and M87: the microtubule-binding domain (MTBD), microtubule-interacting and endosomal-trafficking (MIT) domain, and the AAA domain. The MIT domain of spastin interacts with increased sodium tolerance 1 (IST1) (Allison et al., 2013), and spastin is recruited by IST1 into the endosomal sorting complex required for transport (ESCRT) complex to promote the fission of the recycling tubules from the endosome. The MIT domain of spastin binds to the C-terminal of chromatin-modifying protein/charged multivesicular body protein 1B (CHMP1B) through a series of unique hydrogen bond interactions that recruit spastin to the midbody, thereby promoting cell division (Yang et al., 2008). Both IST1 and CHMP1B belong to ESCRT complexes, and some studies have reported that ESCRT proteins are co-opted by the HIV-1 Gag to assist in viral particle assembly and release of infectious virions (Gupta et al., 2020; Rose, 2021; Rose et al., 2020). We hypothesized that spastin may be involved in the regulation of the HIV-1 life cycle through the ESCRT pathway. The aim of this study was to reveal the specific mechanism by which spastin affects HIV replication.

2. Materials and methods

2.1. Cell culture and transfection

TZM-bl cells were obtained from the NIH AIDS Research and Reference Reagent. HeLa and HEK293T cells were purchased from the American Type Culture Collection (ATCC). All of the above cells were cultured in Dulbecco's Modified Eagle Medium (DMEM, Gibco, Grand Island, USA) supplemented with 10% fetal bovine serum (FBS), 0.1% penicillin, and 0.1% streptomycin at 37 °C and 5% CO_2. Transfection of cells with plasmids or siRNAs was performed using Lipofectamine 3000 Reagent (Invitrogen) according to the manufacturer's protocol. Plasmid DNA concentration was 2 μg/mL and siRNA concentration was 80 nmol/L in each well of a 12-well plate.

2.2. Plasmids and siRNA reagents

The plasmids, pNL4.3, pNL4.3ΔEnvEGFP, and pVSV-G, were kindly provided by Charles Wood (University of Nebraska, Lincoln, USA). The plasmids of HIV-1 Gag-iGFP, which derived from pNL4-3 carries green fluorescent protein (GFP) inserted into the Gag protein between the MA and CA domains of Gag (Chen et al., 2007; Hubner et al., 2007), was provide by Benjamin Chen (Mount Sinai School of Medicine, New York, USA). Three small interfering RNAs (siRNAs) targeting human *spastin*, *CHMP1B*, and *IST1* genes individually were designed and synthesized by GenePharma (Shanghai, China). Non-targeting siRNA was used as a negative control (NC). The M87-spastin fragment was amplified from cDNA and inserted into the expression plasmid pCMV-Tag2B by restriction endonuclease digestion with *BamH*I and *Hind*III, yielding plasmid pM87. Plasmids pM87ΔMIT and pM87ΔMTBD were generated using a Quik Change Site-Directed Mutagenesis Kit (Stratagene). Primers used were as follows: pM87-forward: 5′-GCTGGATCCATGGCAGCCAAGAGGAGCT CCT-3′, pM87-reverse: 5′-GCTAAGCTTTTAAACAGTGGTATCTCCAAA GTCCT-3′; pM87ΔMIT-Forward: 5′-GAGAAGATGCAACCAGTTTTG-3′, pM87ΔMIT-reverse: 5′-GAAGACTCGGACGCGCTC-3′; and pM87 ΔMTBD-forward: 5′-GAAATTGTGGACAATGGAACAG-3′, pM87ΔMTBD -reverse: 5′-GTAACTAGGTGCTCTATGGTGG-3′. Construction of siRNA-restricted pM87 plasmid was commissioned by Sangon Biotech (Shanghai) Co., Ltd. All constructs were confirmed by DNA sequencing.

2.3. Retrovirus production and infection

HIV-1 was produced by pNL4-3 plasmid transfection. HIV-1-VSV-G was produced by transfecting the HIV-1-ΔEnv-EGFP plasmid with pVSV-G. Retroviruses were harvested 48 h after transfection, filtered through a 0.45-μm filter, titered, and stored at −80 °C. For infections, virus was added to cell cultures with diethylaminoethyl (DEAE, 40 μg/mL) and incubated for 48 h. The number of infected cells was determined by X-gal staining.

2.4. Western blot analysis

Whole-cell extracts were prepared by lysing cells, boiling the equivalent protein content in sodium dodecyl sulfate sample buffer, resolution by SDS/PAGE, and transfer to an Immobilon-P membrane (Millipore, Germany). The membranes were incubated with primary antibodies, mouse anti-β-actin (sc-47778, Santa Cruz Biotechnology, Inc. USA, 1:5000), mouse anti-p24 (ab63917, Abcam, USA, 1:2500), rabbit anti-Spasitn (ab31850, Abcam, USA, 1:1000), rabbit anti-CD4 (19068-1-AP, Proteintech Group, Inc. USA, 1:1000), rabbit anti-CHMP1B (14639-1-AP, Proteintech Group, Inc. USA, 1:2000), and rabbit anti-IST1 (51002-1-AP, Proteintech Group, Inc. USA, 1:5000), mouse anti-FLAG (F1804, Sigma-Aldrich, USA, 1:5000) followed by the horseradish peroxidase (HRP)-conjugated anti-rabbit IgG (W4011, Promega, USA, 1:10000) or anti-Mouse IgG secondary antibodies (W4021, Promega, USA, 1:10000). Immunoreactive proteins were detected using an enhanced chemiluminescence kit (Millipore, Germany). The intensities of Western blot bands were quantified using digital images and Image J software after subtraction of the background.

2.5. Real-time quantitative PCR

Total RNA was isolated from cultured cells using an Eastep Total RNA Extraction Kit (Promega) according to the manufacturer's protocol. Then, total RNA was reverse transcribed using a TransScript First-Strand cDNA Synthesis Kit (TransGen Biotech). Real-time quantitative PCR was performed using TransStart Green qPCR SuperMix (TransGen Biotech) in a Real-Time quantitative PCR Detection System (Bio-Rad IQ2). A melting curve analysis was performed to ensure the amplification of a single product. All primers for cDNA amplification of various target genes were designed and optimized using Oligo 7.0 software (Molecular Biology Insights, West Cascade, CO, USA) and synthesized by Sangon Biotech (Shanghai, China). The relative expression levels of the target genes were calculated by normalizing the cycle threshold (Ct) values of the target gene to the Ct values of GAPDH (ΔCt) and determined using the $2^{-\Delta\Delta Ct}$ method.

2.6. Measuring integrated proviral DNA contents

TZM-bl cells were transfected with siRNAs as described above. Total DNA from infected TZM-bl cells was extracted using a DNeasy Blood and Tissue Kit (Qiagen) according to the manufacturer's instructions. Two hundred nanograms of DNA was subjected to the first round of PCR with primers Alu-forward 5′-GCCTCCCAAAGTGCTGGGATTACAG-3′ and HIV-1 Gag-reverse 5′-GTTCCTGCTATGTCACTTCC-3′. After 15 cycles of amplification, DNA products were quantified by real-time quantitative PCR (Lee et al., 2018) using primers targeting HIV-1 Gag (forward, 5′-TGCATGGGTAAAAGTAGTAGAAGAGA-3′; reverse, 5′-TGA-TAATGCTGAAA ACATGGGTA-3′). HIV-1 integrase inhibitor raltegravir (HY-10353, MedChemExpress, New Jersey, USA) was used as a positive control.

2.7. Release efficiency

Cells were transfected with the indicated siRNAs for 72 h and then infected with HIV-1_{NL4-3}. Cells and virus were harvested 48 h later.

Inhibition of the release of virus particles was analyzed in cell lysates and extracellular virions were identified using HIV-1 Gag antibody. Virus release efficiency was calculated as the amount of virion p24 divided by the total amount of Gag (cell $Pr55^{Gag}$ + cell p24 + virion p24).

2.8. Proteasomal and lysosomal inhibition

Cells were transfected with the indicated siRNAs and then with pNL4-3 72 h later. After 24 h, the cells were treated with 5 μmol/L MG132 or 10 μmol/L buffithromycin A1 (Baf-A1) for 18 h. Cell lysates were immunoblotted with anti-p24 or anti-β-actin antibodies as described above.

2.9. Fluorescence microscopy assay for co-localization

HeLa cells were transfected with the siRNAs of spastin for 72 h and then transfected with HIV-1 Gag-iGFP for 4 h. After 24 h, the cells were treated with DMSO or 10 μmol/L Baf-A1. After 18 h, the cells were 4% formaldehyde fixed (10 min) and then incubated in 2% BSA/10% FBS in 0.1% PBS-Tween for 1 h to permeabilise the cells and block non-specific protein-protein interactions. The cells were then incubated with the antibody (LAMP-1, 1 μg/mL) overnight at 4 °C. The antibody of LAMP-1 (sc-18821 AF647, Santa Cruz Biotechnology, Inc., Dallas, USA, 1:500) is conjugated to Alexa Fluor® 647. DAPI (sc-3598, Santa Cruz Biotechnology, Inc., Dallas, USA, 1:10000) was used to stain the nucleus at a concentration of 1 μmol/L. Cells were imaged using a laser scanning confocal microscope (FV1000) with a 60 objective. Each image was obtained using identical microscope settings, including laser power, gain, and contrast. To provide quantitative co-localization of immunofluorescent signals, colocalization coefficients were obtained by using the Image-Pro Plus.

2.10. Statistical analysis

Data were expressed as the mean ± standard deviation. The significance of differences was evaluated using one-way ANOVA or Student's *t*-test in Graphpad Prism 8.0 software. *P* values of ≤ 0.05 were considered significant (*); *P* values ≥ 0.05 (#) were not considered significant.

3. Results

3.1. Spastin is required for the efficient production of new HIV-1 virions in HIV-1 permitted TZM-bl cells

To investigate the effect of spastin on HIV-1 replication, we designed an experiment as shown in Fig. 1A. The TZM-bl cells, which express CD4 and CCR5/CXCR4, were employed in this study. Firstly, the spastin was knocked down by siRNA in TZM-bl cells (Supplementary Fig. S1A). Then, the TZM-bl cells were infected with HIV-1_{NL4-3} at a multiplicity of infection (MOI) of 0.1. After 48 h, culture supernatant and TZM-bl cells were collected, and the virions and intracellular viral proteins were detected using Western blotting. The results showed that knockdown spastin reduced intracellular HIV-1 Gag expression and virions yield by about half (Fig. 1B–D). To further verify our results, we constructed a plasmid expressing the isoform of spastin M87 (named pM87), which is more widely expressed and has more microtubule-severing activity than M1. The TZM-bl cells were transfected with plasmid pM87 and the intracellular Gag expression levels and virions yield were determined at 48 h of post-infection. The results showed that the up-regulation of spastin increased Gag production in both intracellular and HIV-1 virions (Fig. 1E–G) by approximately three times. Meanwhile, TZM-bl cells were co-transfected with siRNAs and siRNA-restricted M87 plasmid (pM87R, Supplementary Fig. S1B) for 48 h, and then infected with HIV-1_{NL4-3} at MOI of 0.1. TZM-bl cell and culture supernatant were collected 48 h later. The vector pCMV-Tag2B was used as a negative control. The results showed that the intracellular expression of HIV-1 Gag and virions yield were rescued by using the siRNA-resistant spastin expressor. (Fig. 1H–J).

Finally, to mimic the antiviral effect of interfering with spastin after viral infection, knockdown of spastin in infected cells 24 h after viral infection showed that the expression level of HIV-1 Gag and virions production were reduced at day 2 and 4 after transfection (Fig. 2A–C). The above results suggested that spastin facilitates HIV-1 replication and virions packaging.

3.2. Spastin knockdown moderately affects the wild-type (WT) HIV-1 infection

Next, we tried to verify the effect of spastin on HIV-1 infection. The spastin-knocking down TZM-bl cells were infected with WT HIV-1_{NL4-3} virus for 4 h and then the number of infected cells was measured by X-Gal staining 48 h after infection. The virus infected NC TZM-bl cells were used as negative control, and heat inactivated virus infected NC TZM-bl cells were used as positive control. The results showed that knocking down spastin reduced the number of HIV-1-infected cells by about 20% compared with the negative control, suggesting that the knockdown of spastin suppressed viral infection (Fig. 2D). Vesicular stomatitis virus glycoprotein (VSV-G)-pseudotyped HIV-1 virus has been widely used in various studies to test the virus production in a single round of replication instead of the multiple rounds of replication-dependent on the HIV-1 envelope exclusively. Here, it was also applied in this experiment. In contrast to WT HIV-1, spastin knockdown didn't affect VSV-G-pseudotyped HIV-1 infection (Fig. 2D). As shown above, our results show that spastin moderately affects HIV-1 infection and is specifically associated with WT HIV-1.

3.3. Spastin knockdown does not impact HIV-1 DNA integration into host cell DNA

Following fusion, retroviral particles subsequently move in a dynein-dependent manner along microtubules to the nucleus, with uncoating and reverse transcription thought to occur during microtubule-dependent trafficking or upon arrival in the nucleus (Arhel et al., 2006, 2007; Su et al., 2010). Considering spastin severs the cytoskeleton microtubules, we next examined the level of viral DNA integration into the host cell DNA to address whether the efficiency of viral transport into the nucleus is affected by microtube-severing ability of spastin. To ensure the accuracy of the detection of virus integration efficiency, the virus needs to infect different groups of cells with the same infection efficiency. Therefore, in order to eliminate the effect of spastin on virus infection (Fig. 2D), VSV-G-pseudotyped HIV-1 virus was used as the infection virus to control infection efficiency for the integration measurement. The spastin knocking down TZM-bl cells were infected with VSV-G-pseudotyped HIV-1 virus (MOI = 0.1) for 4 h. After 24 h of infection, total cells were collected. Nested Alu-PCR was used to quantify the integrated HIV-1 DNA. The results showed that there was no significant difference in integrated viral DNA between the spastin knockdown group and the NC group (Fig. 2E). It suggests HIV integration is not affected by the depletion of spastin.

3.4. Spastin affects intracellular Gag protein yield but does not affect transcription of the gag gene

Spastin is mainly distributed in cytoplasm, as well as partially localized to the nucleus (Sakoe et al., 2021). It has been reported that spastin enters the nucleus through nuclear localization signal (NLS) and binds to the transcription factor HOXA10, forming a complex that binds the empty spiracles homeobox 2 (EMX2) promoter, thereby inhibiting the expression of EMX2 (Daftary et al., 2011). Moreover, HOXA10 competes with STAT3 for binding of the hepatitis B virus X promoter to repress HBV transcription (Yang et al., 2019). However, whether spastin binds to HOXA10 to regulate HIV-1 transcription remains unclear. To determine

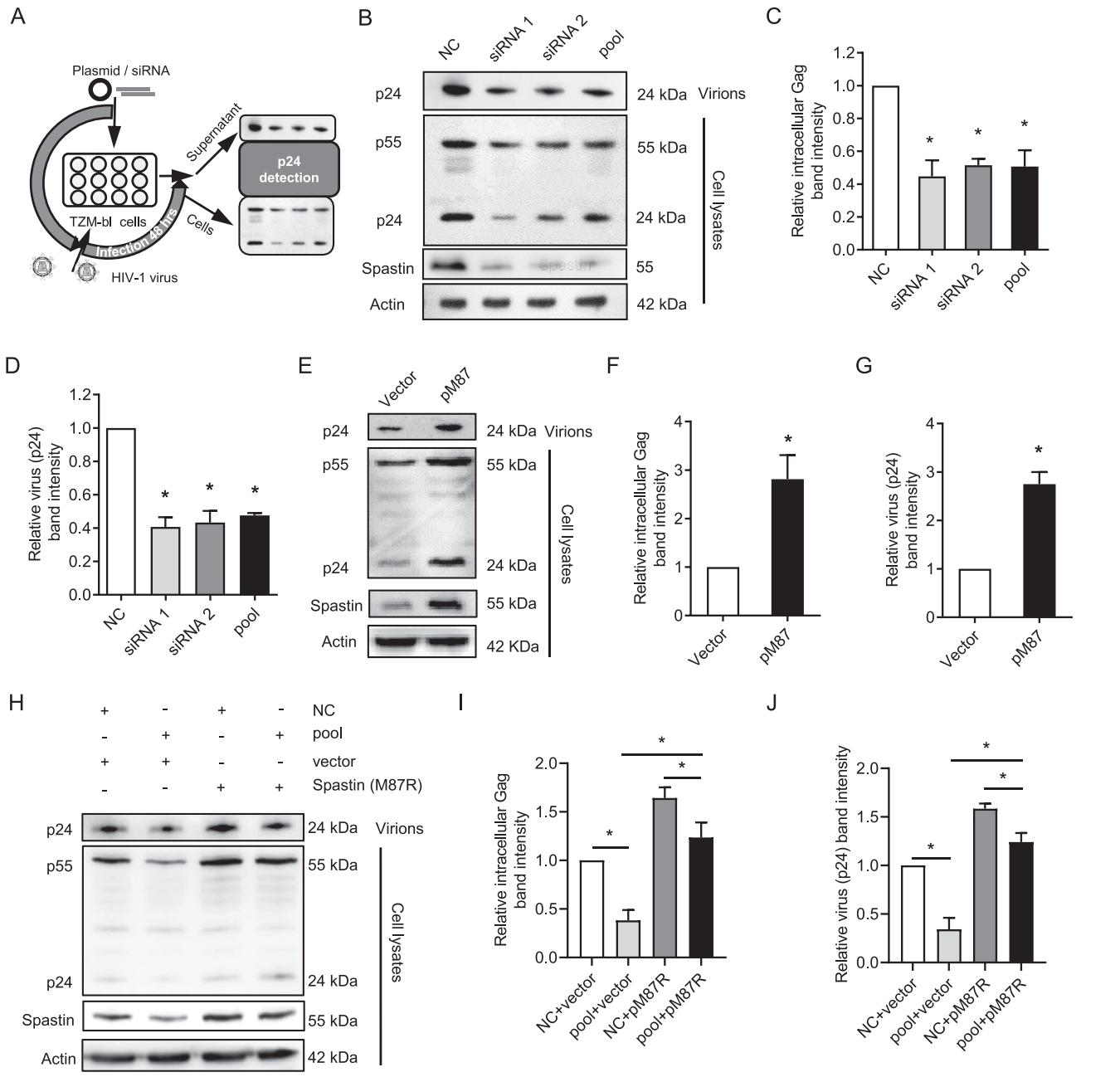

Fig. 1. Spastin affects HIV-1 production. **A** Schematic representation of the experimental design. **B–D** TZM-bl cells were transfected with spastin siRNAs (80 nmol/L) or pool (80 nmol/L, mixture of siRNA1 and siRNA2 with 1:1 ratio) in a 12-well plate and cultured for 72 h. Subsequently, the wild-type HIV-1_{NL4-3} virus (MOI = 0.1) were added to cells and infected for 4 h. After 48 h of infection, the culture supernatant was collected and the cells were lysed. Intracellular viral Gag protein (p55) levels were determined by Western blotting. Relative production of virions was determined by p24 Western blotting. NC: TZM-bl cells transfected with non-targeting siRNA and infected by the wild-type HIV-1_{NL4-3} virus. **E–G** The TZM-bl cells were transfected with the pM87 plasmids (2 μg/mL per 1×10^5 cells), and then the cells were infected with HIV-1_{NL4-3} at the MOI of 0.1. The intracellular Gag expression levels and virions yield were determined by Western blotting at 48 h of post-infection. **H–J** Spastin rescue experiment. The TZM-bl cells were co-transfected with siRNA pool (80 nmol/L, mixture of siRNA1 and siRNA2 with 1:1 ratio) and siRNA-restricted M87 plasmid (pM87R, 2 μg/mL per 1×10^5 cells) for 48 h, and then infected with HIV-1_{NL4-3} at MOI of 0.1. Vector: pCMV-Tag2B, as negative control. NC: TZM-bl cells transfected with non-targeting siRNA and infected by the wild-type HIV-1_{NL4-3} virus. The intracellular viral protein levels were determined by Western blotting. Each experiment was repeated three times. Data presented as the mean ± SD. Student's *t*-test was used for comparison between two groups, and one-way ANOVA was used for comparison between multiple groups *P* values of ≤0.05 were considered significant (*).

the impact of spastin on viral transcription and virions production, spastin knocking down HeLa cells were transfected with pNL4-3 proviral DNA, and the mRNA and intracellular viral protein level were determined at 48 h post transfection. There was no difference in mRNA levels of Gag between the spastin knockdown groups and NC group, indicating that spastin does not impact viral gene transcription (Supplementary Fig. S1C). The effect of spastin on virions production was also analyzed by p24 expression level. The results showed that spastin depletion significantly reduced the production of HIV-1 intracellular Gag by 50% and new virions by about 60% (Supplementary Figs. S1D–F).

To exclude the possibility that cell lineage affected these results, HEK293T cells were also used to repeat the experiment that the effects of spastin on intracellular Gag and mRNA levels. Consistent with the results in HeLa cells, spastin depletion did not affect HIV-1 *gag* transcription

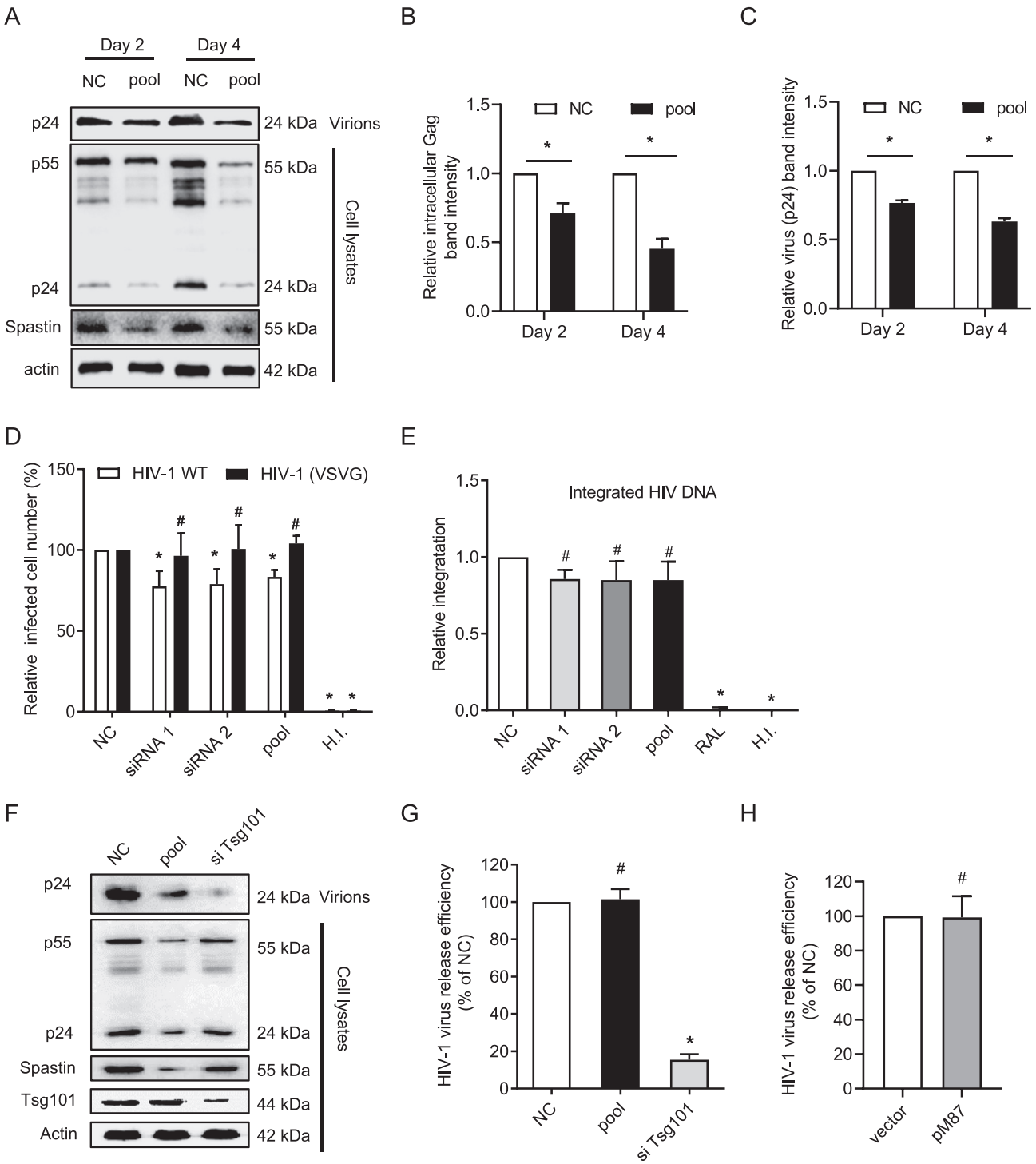

Fig. 2. Spastin affects HIV-1 production but does not affect early events in the HIV-1 life cycle. **A–C** TZM-bl cells in a 12-well plate were infected by wild-type HIV-1 NL4-3 virus (MOI = 0.1) for 4 h. Spastin pool siRNAs (80 nmol/L, mixture of siRNA1 and siRNA2 with 1:1 ratio) or non-targeting siRNA (NC) were transfected into HIV-1-infected TZM-bl cells, and intracellular viral Gag protein levels and virions yield were detected by Western blotting at day 2 and 4 post-transfection. **D** TZM-bl cells in a 12-well plate were transfected with spastin siRNAs or non-targeting siRNA (NC) and cultured for 72 h. Then, WT HIV-1 or VSV-G-pseudotyped HIV-1 virus were added to the cells for 4 h and cultured for 48 h after infection. Heat inactivated virus (H.I.) were used as negative controls. The number of infected cells was determined by X-gal staining. The analyze particles function of Image J was used to count the number of staining cells. **E** VSV-G-pseudotyped HIV-1 virions were added and the inoculated cells were incubated for 24 h. Heat inactivated virus (H.I.) and integrase inhibitor raltegravir (RAL, 30 nmol/L) were used as negative controls. After 24 h, the total cellular DNA was isolated from virus-infected cells. Integrated HIV-1 DNA was quantified by nested Alu-PCR. The numbers of infected cells and integrated HIV-1 DNA in siRNA-transfected cells were normalized to NC siRNA-transfected cells and reported as mean (±SEM) of three independent experiments. **F–H** Spastin is not required for HIV-1 budding. **F** HIV-1 infected TZM-bl cells transfected with spastin siRNA. 48 h later, supernatant was collected, the cells were lysed, and p24 was detected by Western blotting. Tsg101 was used as a positive control. **G** Virus release efficiency was calculated as the amount of virions p24 divided by the total amount of Gag (cellular Pr55Gag + cellular p24 + virion p24). **H** The release efficiency of the overexpressed spastin virus was calculated according to Fig. 1E. Each experiment was repeated three times. Data presented as the mean ± SD. Student's *t*-test was used for comparison between two groups, and one-way ANOVA was used for comparison between multiple groups. *P* values of ≤0.05 were considered significant (*); *P* values ≥ 0.05 (#) were not considered significant.

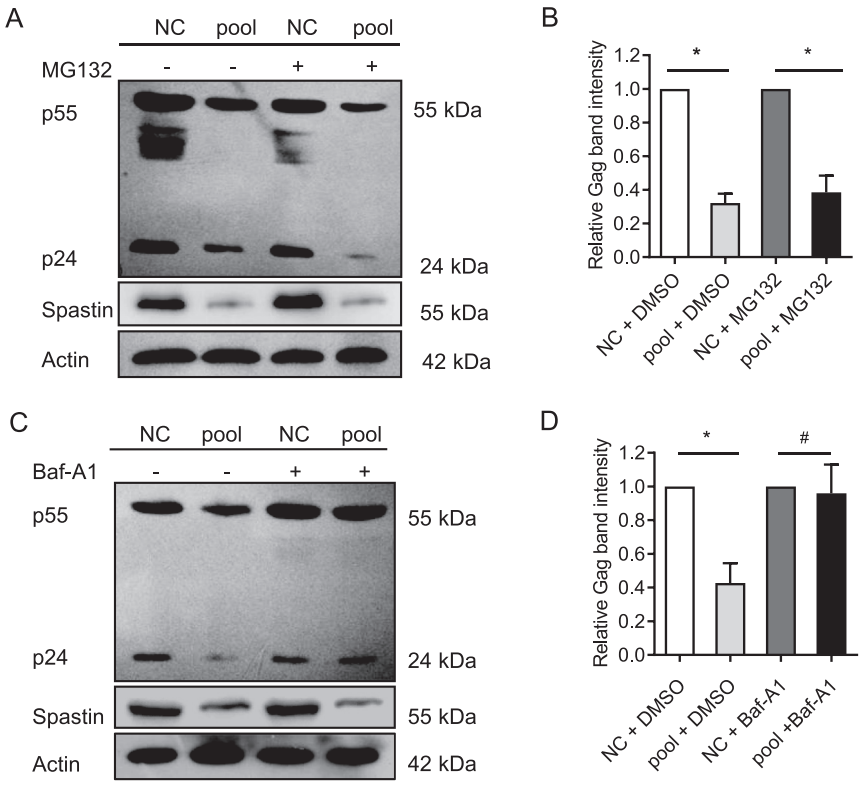

Fig. 3. Spastin is required to sort Gag away from the lysosomal degradation pathway. HeLa cells were transfected with 80 nmol/L pool siRNAs (mixture of siRNA1 and siRNA2 with 1:1 ratio) and then infected with HIV-1_{NL4-3} (MOI = 0.1) 72 h later. After 24 h, the cells were treated with vehicle (DMSO), (**A, B**) MG132 (5 μmol/L), or (**C, D**) Baf-A1 (10 μmol/L) for 18 h. Cell lysates were immunoblotted with anti-p24 or anti-β-actin antibodies. Gag band densities were quantified and the mean densities in three independent experiments were plotted. The Gag band intensities in siRNA-transfected cells were normalized to those of NC siRNA-transfected cells. Each experiment was repeated three times. Data presented as the mean ± SD. Student's *t*-test was used for comparison between two groups, and one-way ANOVA was used for comparison between multiple groups. *P* values of ≤0.05 were considered significant (*); *P* values ≥ 0.05 (#) were not considered significant.

(Supplementary Fig. S1G) but reduced the production of HIV-1 intracellular Gag by 50% and new virions by about 60% (Supplementary Figs. S1H–J). In contrast, overexpression of spastin in HeLa cells enhanced the level of HIV-1 intracellular Gag (Supplementary Figs. S2A and S2B). Notably, the highest concentration of spastin (2 μg/mL per 1×10^5 cells) increased the intracellular Gag production by 2.4 times. We repeated with an irrelevant plasmid (pEGFP-C1) to validate the results, and spastin didn't have any effect on HIV-1 intracellular Gag production (Supplementary Figs. S2C and S2D). Experiments described in this section suggest that spastin is required for Gag expression.

3.5. Spastin is dispensable for virus budding

During the budding stage of HIV-1 replication, the ESCRT-III complex is recruited by p6 domain from Gag to bend the viral membrane and form a neck-like structure, and then recruit ATPase VPS4 to cleat the viral membrane scission (Hurley and Cada, 2018; Johnson et al., 2018; Meng and Lever, 2021). The ESCRT-III subunit IST1 recruits spastin into ESCRT to promote fission of recycling tubules from the endosome (Allison et al., 2013). The ESCRT-III subunit CHMP1B recruits spastin to the intermediate, which promotes cell division (Yang et al., 2008). Therefore, we hypothesized that spastin may cooperate with the ESCRT-related pathway to participate in the virus budding process. The effects of spastin on virus budding were detected by calculating the virus release efficiency. Virus release efficiency was calculated as the amount of virions p24 divided by the total amount of Gag (cellular $Pr55^{Gag}$ + cellular p24 + virion p24). As shown in Fig. 2F and G, the virus release efficiency of NC group was normalized to 100%, and the virus release efficiency in spastin knockdown group was 101.51%, with no statistical significance. Tsg101 a factor essential for HIV-1 budding (Garrus et al., 2001), was used as a positive control, and the results showed that Tsg101 knockdown reduced the virus release efficiency from 100% to 15.4%. Meanwhile, according to the results of Fig. 1E, we calculated the influence of spastin overexpression on HIV-1 virus budding. As shown in Fig. 2H, spastin overexpression did not promote HIV-1 virus budding. These results suggested that spastin is not required for virus budding.

3.6. Spastin knockdown promotes lysosomal degradation of Gag

Previous studies have shown that spastin helps transferrin receptor (TFNR) escape the lysosomal degradation pathway by interacting with ESCRT-III subunit IST1 to regulate endosomal sorting and tubule division (Allison et al., 2013). We hypothesized that HIV-1 Gag might also take advantage of spastin to escape the lysosomal degradation pathway. Spastin knocking down HeLa cells were transfected with HIV-1_{NL4-3} proviral DNA. Twenty-four hours after transfection, the culture medium was replaced with a drug that disrupted either lysosome function (Baf-A1) or proteasome function (MG132) (Zhang et al., 2021). Western blot analysis of the cell lysates confirmed that knockdown of spastin consistently decreased intracellular Gag concentrations in the presence of the proteasomal inhibitor (Fig. 3A and B). However, this reduction was rescued by treatment with the lysosomal inhibitor Baf-A1 (Fig. 3C and D). It indicated that spastin prevents Gag from entering the lysosomal degradation pathway, which is necessary for HIV-1 efficient replication.

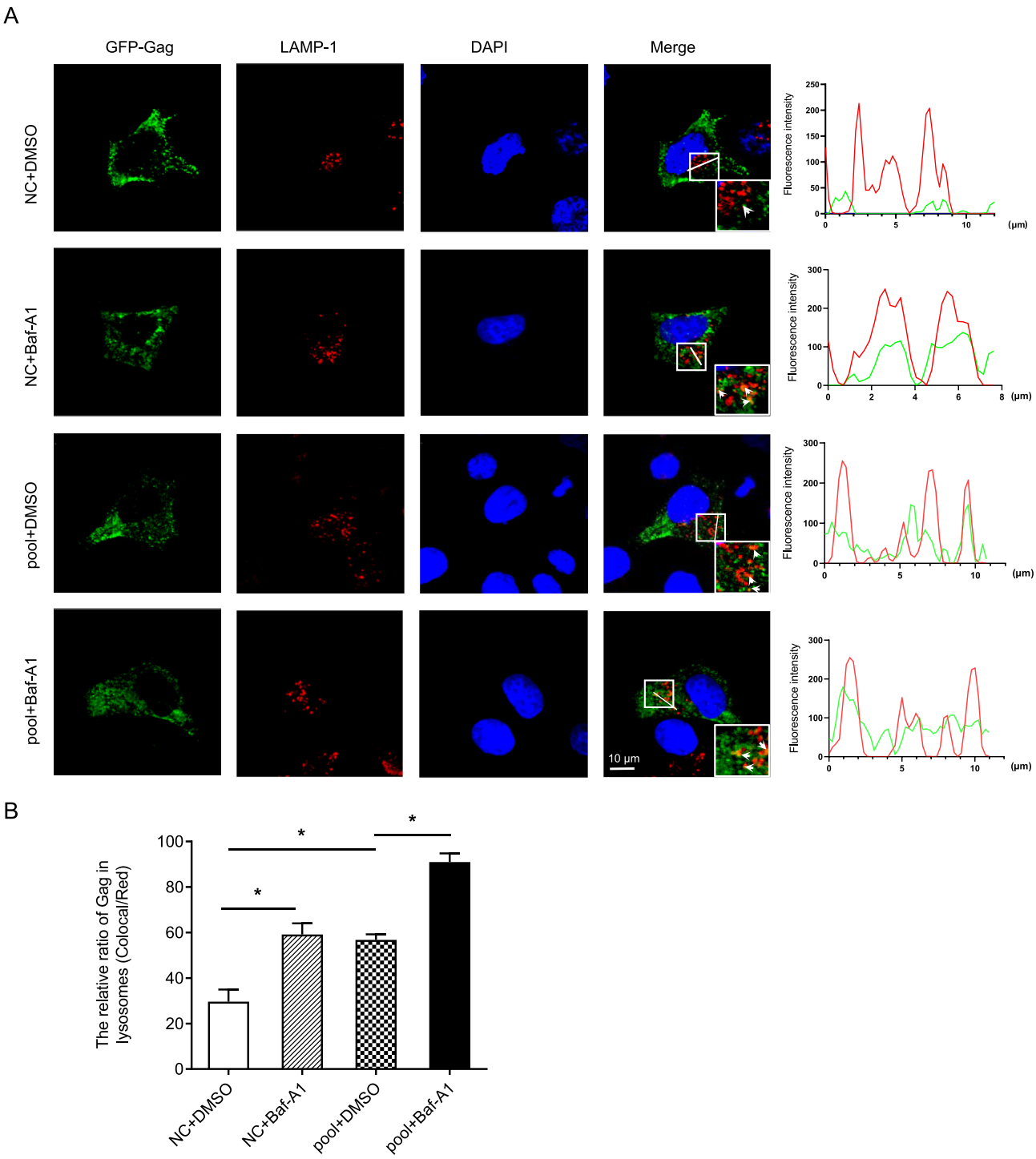

Fig. 4. Spastin knockdown increases Gag and lysosome co-localization. **A** HeLa cells were transfected with the spastin siRNAs (80 nmol/L) and pool siRNAs (mixture of siRNA1 and siRNA2 with 1:1 ratio) in a 12-well plate and cultured for 72 h and then transfected with HIV-1 Gag-iGFP (1 μg/mL) for 4 h. After 24 h, the cells were treated with DMSO or 10 μmol/L Baf-A1. After 18 h, the cells were stained with an antibody for LAMP-1. Representative fluorescent images for each dye were shown. The green signal represents the inserted-GFP Gag, the red signal represents the lysosome staining by LAMP-1 and the blue signal represents the nuclear DNA staining by DAPI. Arrows in boxes point to colocalized puncta. Scale bar: 10 μm. The white line is the fluorescence intensity detection area, which was detected using Image J. **B** Images were analyzed for co-localization in Image Pro Plus. Co-localization coefficient describes the fraction of red channel that overlapped with the green channel. The result showed that spastin's knockdown increases co-localization of Gag and lysosome. Furthermore, the co-localization of Gag and lysosome was enhanced by Baf-A1 treatment. Each experiment was repeated more than three times. *P* values of ≤0.05 were considered significant (*).

3.7. Spastin knockdown increases Gag and lysosome co-localization

To further prove that spastin prevents Gag from entering the lysosomal degradation pathway, the localization of Gag and lysosome was detected by immunofluorescence. Spastin down-regulated HeLa cells were transfected with HIV-1 Gag-iGFP for 4 h. HIV-1 Gag-iGFP has been reported that the inserted-GFP does not affect the transport of Gag (Chen et al., 2007; Hubner et al., 2007). After 24 h, the cells were treated with DMSO or 10

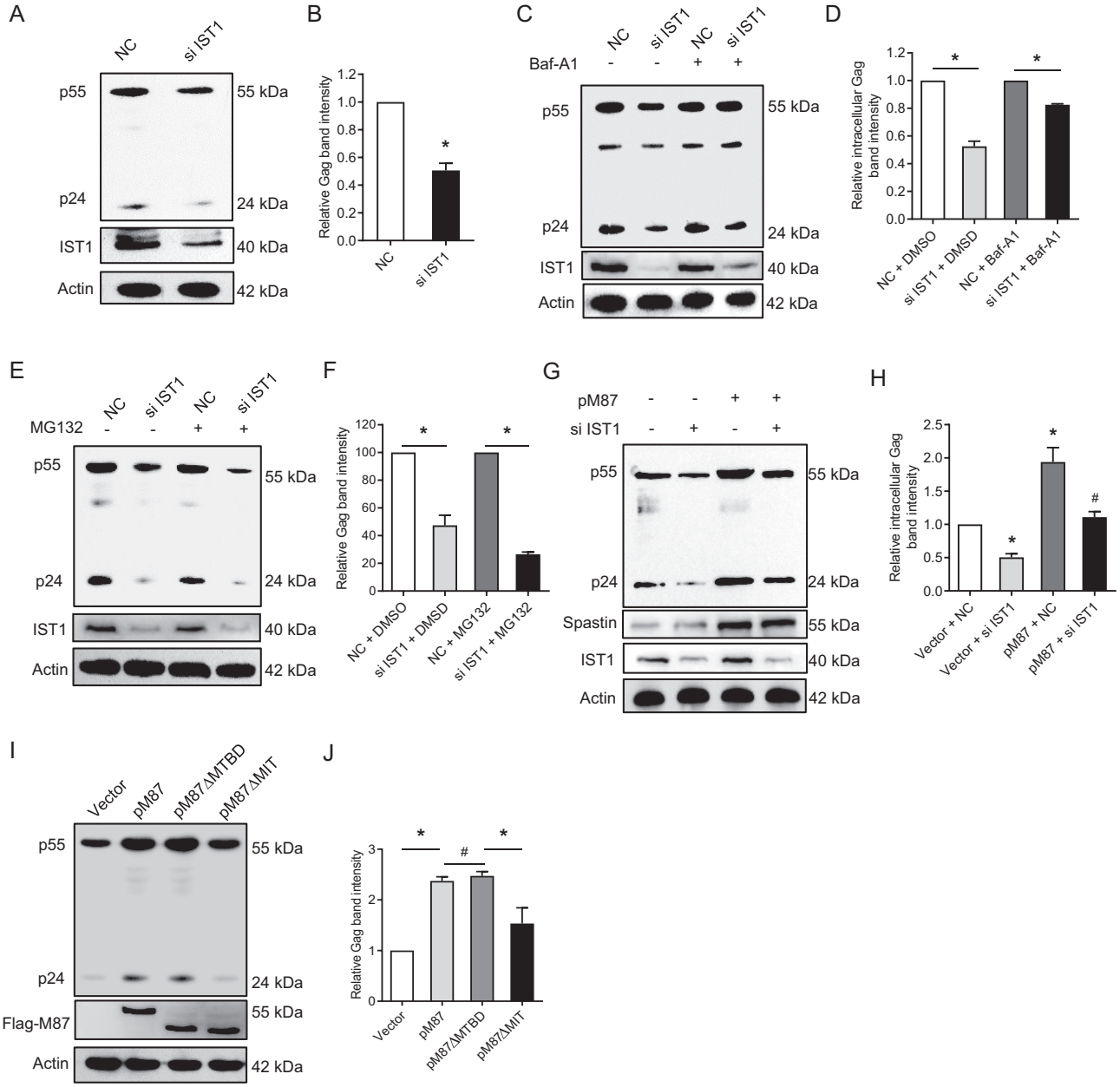

Fig. 5. Spastin keeps Gag away from the lysosomal degradation pathway by cooperating with IST1. **A, B** IST1 depletion reduces intracellular viral Gag levels. HeLa cells were transfected with the indicated IST1 siRNA (80 nmol/L) in a 12-well plate and cultured for 72 h and then transfected with pNL4-3 for 4 h. Cells were harvested after 48 h. The levels of endogenous IST1 and intracellular viral Gag protein were quantified by Western blotting. **C, D** The siIST1-transfected HeLa cells transfected with pNL4-3 were treated with vehicle (DMSO) or 10 μmol/L Baf-A1 and then immunoblotted using the antibodies indicated. **E, F** The siIST1-transfected HeLa cells transfected with pNL4-3 were treated with vehicle (DMSO) or 5 μmol/L MG132 and subsequently immunoblotted using the antibodies indicated. **G, H** HeLa cells transfected with siRNA against IST1 for 72 h and then were co-transfected with pNL4-3 and pM87 or the vector. Intracellular viral Gag protein levels were monitored by Western blotting. **I, J** Cells were co-transfected with constant amounts of HIV-1 pNL4-3 (1 μg/mL) and a pM87 or pM87 deletion mutant plasmid (pM87ΔMTBD/pM87ΔMIT) (2 μg/mL per 1×10^5 cells). Cells were harvested after 48 h. Intracellular viral Gag protein levels were monitored by Western blotting. Anti-Flag antibodies were used to detect M87 and the deletion mutant M87. Each experiment was repeated three times. Data presented as the mean ± SD. Student's *t*-test was used for comparison between two groups, and one-way ANOVA was used for comparison between multiple groups. *P* values of ≤0.05 were considered significant (*); *P* values ≥ 0.05 (#) were not considered significant..

μmol/L Baf-A1 for 18 h and then stained with antibodies recognizing markers of the lysosomal compartments. The results showed that the co-localization of lysosome and Gag in NC group was about 30%, however, the co-localization of lysosome and Gag protein increased from 30% to 60% in the spastin knockdown group. Furthermore, when lysosomal inhibitor was added, the co-localization of NC group and spastin knockdown group increased from 30% to 50.74% and from 60% to 90.97%, respectively. (Fig. 4). These results verified that spastin knockdown promotes lysosomal degradation of Gag.

3.8. ESCRT protein IST1 is involved in spastin regulation of lysosomal degradation of Gag

As described above, spastin regulates endosome sorting and tubule division by interacting with ESCRT-III subunit IST1, assist in TFNR escape the lysosomal degradation pathway (Allison et al., 2013). Next, we tested whether IST1 knockdown affected Gag degradation. IST1 knockdown did reduce the total intracellular Gag concentration by 50% (Fig. 5A and B), and this reduction was partially rescued by lysosomal

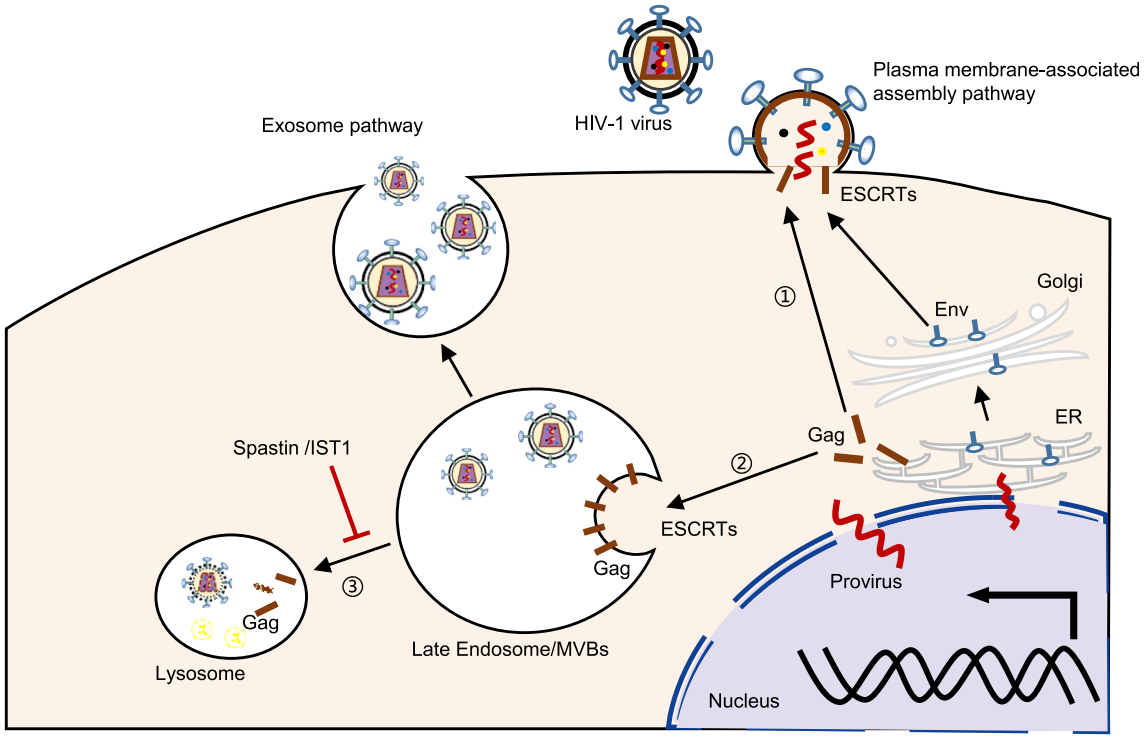

Fig. 6. Spastin regulates lysosomal degradation of intracellular Gag by specifically interacting with the ESCRT protein IST1. ① After the synthesis of HIV-1 Gag, part of the Gag protein is directly transported to the cell membrane for viral assembly, budding and release. ② The other part is transported to the late endosome/multivesicular bodies (MVBs) (Molle et al., 2009; Sherer et al., 2003) and released by the viral exosomal pathway (Balasubramaniam and Freed, 2011; Booth et al., 2006; Kramer et al., 2005; Nguyen et al., 2003). ③ If the late endosomes/MVBs fuse with lysosomes, the internal proteins will be degraded. By interacting with increased sodium tolerance 1 (IST1), spastin inhibited the entry of HIV-1 Gag into the lysosomal degradation pathway. ER, endoplasmic reticulum; ESCRT, endosomal sorting complex required for transport.

inhibitor Baf-A1, restoring intracellular Gag concentration to 82% of the NC group (Fig. 5C and D), but not by the proteasome inhibitor MG132 (Fig. 5E and F). To further understand the involvement of IST1 in spastin-mediated Gag degradation, the IST1 knocked down HeLa cells were co-transfected with pNL4-3 and pM87. The results showed that knockdown of IST1 counteracted the increase of intracellular Gag levels in HeLa cells that overexpressing spastin (Fig. 5G and H), suggesting that IST1 plays a role in spastin regulation of Gag degradation. We also found that CHMP1B, another ESCRT protein interacting with spastin, also affects the concentration of Gag (Supplementary Figs. S2E and S2F). However, knockdown of CHMP1B did not counteract intracellular Gag concentrations in spastin-overexpressing cells (Supplementary Figs. S2G and S2H). These results suggest that spastin regulates lysosomal degradation of intracellular Gag by interacting with IST1 rather than with CHMP1B.

3.9. Spastin cooperates with IST1 to regulate Gag degradation

IST1 promotes the fission of recycling tubules from the endosome by interacting with the MIT domain of spastin and recruiting spastin to the ESCRT complex (Allison et al., 2013). To examine whether spastin binding to IST1 was required for spastin to regulate Gag degradation, we constructed the MIT-domain deletion plasmid and constructed a MTBD-domain deletion plasmid as a control. The results showed that WT spastin consistently improved the level of intracellular HIV-1 Gag, while spastin without MIT domain failed to increase the level of intracellular HIV-1 Gag (Fig. 5I and J). However, spastin without MTBD domain increased the level of intracellular HIV-1 Gag as well as WT spastin. As shown in Fig. 5I, the molecular weight of spastin with domain deletion decreased, but its protein expression level was not significantly affected. The data suggest MIT domain is required for efficient retention of intracellular Gag presumably by interacting with IST1, whereas the MTBD is not required.

4. Discussion

The protein spastin is encoded by the *SPAST* gene, which was first identified as a mutation of spastin that causes hereditary spastic paraplegia in humans (Hazan et al., 1999; Mereaux et al., 2022). It plays a role in axon growth and arborization in neurons (Evans et al., 2005; Jeong et al., 2019). In zebrafish, spastin knockdown leads to shorter spinal motor neuron axons (Butler et al., 2010). Spastin was found to be necessary for HIV-1 efficient replication (Brass et al., 2008), but the mechanism underlying this relationship is not completely clear to date. The aim of this study was to investigate the mechanism by which spastin affects HIV-1 replication.

By studying the effect of spastin on the replication cycle of HIV-1, we found that spastin knockdown reduces the infection of the WT HIV-1 virus approximately 17%–22% with significant difference, but doesn't affect the VSV-G-pseudotyped HIV-1 virus infection. HIV-1 entry is carried out by Env-mediated membrane fusion. First, HIV-1's Env binds to host CD4, which leads to conformational changes in Env, and subsequently, the V3 loop of Env binds to co-receptors, such as CXCR4 and CCR5 (Wilen et al., 2012). The G protein of VZV mediates virus entry by endocytosis, which is different from HIV-1 Env-mediated membrane fusion (Yu et al., 2009). Allison et al. found that spastin regulates receptor sorting, preventing degradation and sorting of receptors into the recycling pathway (Allison et al., 2013). As a receptor for HIV-1 binding, CD4 may affect HIV-1 infection if it is regulated by spastin. However, we found no effect of spastin depletion on CD4 degradation (Supplementary Figs. S2I and S2J). The entry of HIV-1_{NL4-3} virus requires the CXCR4 co-receptor. Yoder and colleagues examined the ability of X4-tropic HIV-1 to infect resting $CD4^+$

T cells and found that HIV-1-mediated, $G_{\alpha i}$ signaling through CXCR4 was required for entry (Yoder et al., 2008). This pathway triggered the activation of a cellular actin-depolymerizing molecule, cofilin, altering cortical actin dynamics near the cell surface and facilitating viral fusion. We speculate that spastin may affect the expression of co-receptors, which needs to be further studied in the future.

On the other hand, it has been reported that ESCRT-III improves the spread efficiency of human cytomegalovirus (Streck et al., 2018), and we speculate that spastin may promote the spread efficiency of HIV-1 through ESCRT-III pathway. This study provided the direct evidence that spastin affects intracellular Gag levels by controlling lysosomal degradation of Gag (Figs. 3 and 4). In the past decade, it has become increasingly apparent that the process from Gag synthesis to assembled capsids is coordinated and facilitated by host factors. In some cell types, particularly macrophages, HIV-1 particles are known to accumulate primarily in intracellular compartments. Raposo et al. showed that these compartments correspond to multivesicular bodies/late endosomes, which can fuse with the plasma membrane to release mature HIV-1 particles (Raposo et al., 2002). Goff et al. also found that HIV-1 Gag associates with endosomal trafficking compartments (Goff et al., 2003). Our results showed that spastin regulates lysosomal degradation of intracellular Gag by specifically interacting with the ESCRT protein IST1 (Fig. 6). Similar to other findings, it has shown that endogenous spastin is located in the endosome, and the ESCRT-spastin interaction promotes the fission of tubules recovered from the endosome, diverting some receptor proteins away from the lysosomal degradation pathway (Allison et al., 2013).

In our study, it was found that spastin did not affect the budding of HIV-1. VPS4 and spastin belong to the AAA ATPase family, but the role in viral replication is different. VPS4 provides necessary energy and completes virus-cell membrane fission by hydrolyzing ATP during virus budding (Gupta et al., 2020; Tavares et al., 2021). Spastin also hydrolyzes ATP and has the effect of severing microfilaments in the last step of cell mitosis (Connell et al., 2009). However, in this study, we found that knockdown of spastin did not affect the efficiency of virus release. This implies that spastin did not participate in the energy supply and microfilament cleavage during viral budding. It has been reported that the ESCRT protein complex is extremely important for virus budding (Morita et al., 2011), such as TSG101 (Garrus et al., 2001), ALIX (Rose et al., 2020) (Ku et al., 2014; Strack et al., 2003), CHMP2A, and CHMP4B (Morita et al., 2011). However, CHMP1B and IST1, which also belong to the ESCRT complex, are not required for HIV-1 budding (Agromayor et al., 2009; Bajorek et al., 2009; Morita et al., 2011). Thus, spastin may not be involved in HIV-1 virus budding through its interaction with CHMP1B or IST1.

There are some limitations of the current study. It should be noted that our results were based exclusively on the widely used laboratory-adapted HIV-1 strain NL4-3 and transformed cell lines. Primary cells and other wild-type HIV-1 strains will be included in future studies to elucidate the detailed mechanism underlying spastin's effects on HIV-1. Whether HIV-1 replication is affected by spastin in physiological conditions is a question need to be addressed. The effect of silencing spastin using siRNA in this paper was not significant, CRISPR/Cas9 approach can be used to knock out spastin at the gene level in our next related paper.

5. Conclusions

In this study, we explored the mechanism by which spastin affects HIV-1 replication. The results showed that spastin was necessary for HIV-1 efficient replication. Spastin regulates the lysosomal pathway by interacting with ESCRT protein IST1, and maintains intracellular HIV-1 Gag concentration by preventing Gag from lysosomal degradation.

Data availability

All the data generated during the current study are included in the manuscript. The raw data supporting the conclusions of this article will be made available by the authors, without undue reservation.

Ethics statement

This article does not contain any studies with human or animal subjects performed by any authors.

Author contributions

Wenyuan Shen: Investigation, methodology, formal analysis, validation. Chang Liu: Methodology, supervision, funding acquisition. Yue Hu: Validation, supervision. Qian Ding: Methodology, validation. Jiabin Feng: Conceptualization, validation. Zhou Liu: Investigation, supervision. Xiaohong Kong: Conceptualization, funding acquisition, project administration, writing - reviewing and editing.

Conflict of interest

The authors declare that they have no conflict of interest.

Acknowledgments

We greatly appreciate Prof. Charles Wood (University of Nebraska, Lincoln, USA) for the gift of the infectious molecular clones (pNL4.3, pNL4.3ΔEnvEGFP, and pVSV-G). We also greatly appreciate Prof. Benjamin Chen (Mount Sinai School of Medicine, New York, USA) for the gift of the infectious molecular clone HIV-1 Gag-iGFP. This study was supported by grants from the National Natural Science Foundation of China (81571987) and Natural Science Foundation of Tianjin Municipal Science and Technology Commission (20JCQNJC01750, 21JCQNJC01600).

Appendix A. Supplementary data

Supplementary data to this article can be found online at https://doi.org/10.1016/j.virs.2023.05.006.

References

Agromayor, M., Carlton, J.G., Phelan, J.P., Matthews, D.R., Carlin, L.M., Ameer-Beg, S., Bowers, K., Martin-Serrano, J., 2009. Essential role of hIST1 in cytokinesis. Mol. Biol. Cell 20, 1374–1387.

Allison, R., Lumb, J.H., Fassier, C., Connell, J.W., Ten Martin, D., Seaman, M.N., Hazan, J., Reid, E., 2013. An ESCRT-spastin interaction promotes fission of recycling tubules from the endosome. J. Cell Biol. 202, 527–543.

Arhel, N., Munier, S., Souque, P., Mollier, K., Charneau, P., 2006. Nuclear import defect of human immunodeficiency virus type 1 DNA flap mutants is not dependent on the viral strain or target cell type. J. Virol. 80, 10262–10269.

Arhel, N.J., Souquere-Besse, S., Munier, S., Souque, P., Guadagnini, S., Rutherford, S., Prevost, M.C., Allen, T.D., Charneau, P., 2007. HIV-1 DNA Flap formation promotes uncoating of the pre-integration complex at the nuclear pore. EMBO J. 26, 3025–3037.

Bajorek, M., Morita, E., Skalicky, J.J., Morham, S.G., Babst, M., Sundquist, W.I., 2009. Biochemical analyses of human IST1 and its function in cytokinesis. Mol. Biol. Cell 20, 1360–1373.

Balasubramaniam, M., Freed, E.O., 2011. New insights into HIV assembly and trafficking. Physiology (Bethesda) 26, 236–251.

Booth, A.M., Fang, Y., Fallon, J.K., Yang, J.M., Hildreth, J.E., Gould, S.J., 2006. Exosomes and HIV Gag bud from endosome-like domains of the T cell plasma membrane. J. Cell Biol. 172, 923–935.

Brass, A.L., Dykxhoorn, D.M., Benita, Y., Yan, N., Engelman, A., Xavier, R.J., Lieberman, J., Elledge, S.J., 2008. Identification of host proteins required for HIV infection through a functional genomic screen. Science 319, 921–926.

Butler, R., Wood, J.D., Landers, J.A., Cunliffe, V.T., 2010. Genetic and chemical modulation of spastin-dependent axon outgrowth in zebrafish embryos indicates a role for impaired microtubule dynamics in hereditary spastic paraplegia. Dis Model. Mech. 3, 743–751.

Chen, P., Hubner, W., Spinelli, M.A., Chen, B.K., 2007. Predominant mode of human immunodeficiency virus transfer between T cells is mediated by sustained Env-dependent neutralization-resistant virological synapses. J. Virol. 81, 12582–12595.

Chiang, K., Sung, T.L., Rice, A.P., 2012. Regulation of cyclin T1 and HIV-1 Replication by microRNAs in resting CD4+ T lymphocytes. J. Virol. 86, 3244–3252.

Connell, J.W., Lindon, C., Luzio, J.P., Reid, E., 2009. Spastin couples microtubule severing to membrane traffic in completion of cytokinesis and secretion. Traffic 10, 42–56.

Daftary, G.S., Tetrault, A.M., Jorgensen, E.M., Sarno, J., Taylor, H.S., 2011. A novel role for the AAA ATPase spastin as a HOXA10 transcriptional corepressor in Ishikawa endometrial cells. Mol. Endocrinol. 25, 1539–1549.

Deluca, G.C., Ebers, G.C., Esiri, M.M., 2004. The extent of axonal loss in the long tracts in hereditary spastic paraplegia. Neuropathol. Appl. Neurobiol. 30, 576–584.
Evans, K.J., Gomes, E.R., Reisenweber, S.M., Gundersen, G.G., Lauring, B.P., 2005. Linking axonal degeneration to microtubule remodeling by Spastin-mediated microtubule severing. J. Cell Biol. 168, 599–606.
Frankel, A.D., Young, J.A., 1998. HIV-1: fifteen proteins and an RNA. Annu. Rev. Biochem. 67, 1–25.
Garrus, J.E., von Schwedler, U.K., Pornillos, O.W., Morham, S.G., Zavitz, K.H., Wang, H.E., Wettstein, D.A., Stray, K.M., Cote, M., Rich, R.L., Myszka, D.G., Sundquist, W.I., 2001. Tsg101 and the vacuolar protein sorting pathway are essential for HIV-1 budding. Cell 107, 55–65.
Ghimire, D., Rai, M., Gaur, R., 2018. Novel host restriction factors implicated in HIV-1 replication. J. Gen. Virol. 99, 435–446.
Goff, A., Ehrlich, L.S., Cohen, S.N., Carter, C.A., 2003. Tsg101 control of human immunodeficiency virus type 1 Gag trafficking and release. J. Virol. 77, 9173–9182.
Gupta, S., Bromley, J., Saffarian, S., 2020. High-speed imaging of ESCRT recruitment and dynamics during HIV virus like particle budding. PLoS One 15, e0237268.
Hazan, J., Fonknechten, N., Mavel, D., Paternotte, C., Samson, D., Artiguenave, F., Davoine, C.S., Cruaud, C., Durr, A., Wincker, P., Brottier, P., Cattolico, L., Barbe, V., Burgunder, J.M., Prud'homme, J.F., Brice, A., Fontaine, B., Heilig, B., Weissenbach, J., 1999. Spastin, a new AAA protein, is altered in the most frequent form of autosomal dominant spastic paraplegia. Nat. Genet. 23, 296–303.
Hubner, W., Chen, P., Del Portillo, A., Liu, Y., Gordon, R.E., Chen, B.K., 2007. Sequence of human immunodeficiency virus type 1 (HIV-1) Gag localization and oligomerization monitored with live confocal imaging of a replication-competent, fluorescently tagged HIV-1. J. Virol. 81, 12596–12607.
Hurley, J.H., Cada, A.K., 2018. Inside job: how the ESCRTs release HIV-1 from infected cells. Biochem. Soc. Trans. 46, 1029–1036.
Jeong, B., Kim, T.H., Kim, D.S., Shin, W.H., Lee, J.R., Kim, N.S., Lee, D.Y., 2019. Spastin contributes to neural development through the regulation of microtubule dynamics in the primary cilia of neural stem cells. Neuroscience 411, 76–85.
Johnson, D.S., Bleck, M., Simon, S.M., 2018. Timing of ESCRT-III protein recruitment and membrane scission during HIV-1 assembly. Elife 7, e36221.
Kramer, B., Pelchen-Matthews, A., Deneka, M., Garcia, E., Piguet, V., Marsh, M., 2005. HIV interaction with endosomes in macrophages and dendritic cells. Blood Cells Mol. Dis. 35, 136–142.
Ku, P.I., Bendjennat, M., Ballew, J., Landesman, M.B., Saffarian, S., 2014. ALIX is recruited temporarily into HIV-1 budding sites at the end of gag assembly. PLoS One 9, e96950.
Kuo, Y.W., Trottier, O., Mahamdeh, M., Howard, J., 2019. Spastin is a dual-function enzyme that severs microtubules and promotes their regrowth to increase the number and mass of microtubules. Proc. Natl. Acad. Sci. U. S. A. 116, 5533–5541.
Lee, W.J., Fu, R.M., Liang, C., Sloan, R.D., 2018. IFITM proteins inhibit HIV-1 protein synthesis. Sci. Rep. 8, 14551.
Li, D., Wei, T., Rawle, D.J., Qin, F., Wang, R., Soares, D.C., Jin, H., Sivakumaran, H., Lin, M.H., Spann, K., Abbott, C.M., Harrich, D., 2015. Specific interaction between eEF1A and HIV RT is critical for HIV-1 reverse transcription and a potential anti-HIV target. PLoS Pathog. 11, e1005289.
Li, S., Zhang, J., Zhang, J., Li, J., Cheng, L., Chen, L., Cha, C., Guo, G., 2021. Spastin interacts with CRMP2 to regulate neurite outgrowth by controlling microtubule dynamics through phosphorylation modifications. CNS Neurol. Disord.: Drug Targets 20, 249–265.
Liu, G.Y., Chen, S.C., Lee, G.H., Shaiv, K., Chen, P.Y., Cheng, H., Hong, S.R., Yang, W.T., Huang, S.H., Chang, Y.C., Wang, H.C., Kao, C.L., Sun, P.C., Chao, M.H., Lee, Y.Y., Tang, M.J., Lin, Y.C., 2022. Precise control of microtubule disassembly in living cells. EMBO J., e110472
Lopes, A.T., Hausrat, T.J., Heisler, F.F., Gromova, K.V., Lombino, F.L., Fischer, T., Ruschkies, L., Breiden, P., Thies, E., Hermans-Borgmeyer, I., Schweizer, M., Schwarz, J.R., Lohr, C., Kneussel, M., 2020. Spastin depletion increases tubulin polyglutamylation and impairs kinesin-mediated neuronal transport, leading to working and associative memory deficits. PLoS Biol. 18, e3000820.
Lumb, J.H., Connell, J.W., Allison, R., Reid, E., 2012. The AAA ATPase spastin links microtubule severing to membrane modelling. Biochim. Biophys. Acta 1823, 192–197.
Ma, X., Chen, T., Peng, Z., Wang, Z., Liu, J., Yang, T., Wu, L., Liu, G., Zhou, M., Tong, M., Guan, Y., Zhang, X., Lin, Y., Tang, X., Li, L., Tang, Z., Pan, T., Zhang, H., 2021. Histone chaperone CAF-1 promotes HIV-1 latency by leading the formation of phase-separated suppressive nuclear bodies. EMBO J. 40, e106632.
Meng, B., Lever, A.M.L., 2021. The interplay between ESCRT and viral factors in the enveloped virus life cycle. Viruses 13, 324.
Mereaux, J.L., Banneau, G., Papin, M., Coarelli, G., Valter, R., Raymond, L., Kol, B., Ariste, O., Parodi, L., Tissier, L., Mairey, M., Ait Said, S., Gautier, C., Guillaud-Bataille, M., French, S.c.n., Forlani, S., de la Grange, P., Brice, A., Vazza, G., Durr, A., Leguern, E., Stevanin, G., 2022. Clinical and genetic spectra of 1550 index patients with hereditary spastic paraplegia. Brain 145, 1029–1037.
Mitra, S., Shanmugapriya, S., Santos da Silva, E., Naghavi, M.H., 2020. HIV-1 exploits CLASP2 to induce microtubule stabilization and facilitate virus trafficking to the nucleus. J. Virol. 94, e00404–e00420.
Molle, D., Segura-Morales, C., Camus, G., Berlioz-Torrent, C., Kjems, J., Basyuk, E., Bertrand, E., 2009. Endosomal trafficking of HIV-1 gag and genomic RNAs regulates viral egress. J. Biol. Chem. 284, 19727–19743.
Morita, E., Sandrin, V., McCullough, J., Katsuyama, A., Baci Hamilton, I., Sundquist, W.I., 2011. ESCRT-III protein requirements for HIV-1 budding. Cell Host Microbe 9, 235–242.
Nguyen, D.G., Booth, A., Gould, S.J., Hildreth, J.E., 2003. Evidence that HIV budding in primary macrophages occurs through the exosome release pathway. J. Biol. Chem. 278, 52347–52354.
Raposo, G., Moore, M., Innes, D., Leijendekker, R., Leigh-Brown, A., Benaroch, P., Geuze, H., 2002. Human macrophages accumulate HIV-1 particles in MHC II compartments. Traffic 3, 718–729.
Riano, E., Martignoni, M., Mancuso, G., Cartelli, D., Crippa, F., Toldo, I., Siciliano, G., Di Bella, D., Taroni, F., Bassi, M.T., Cappelletti, G., Rugarli, E.I., 2009. Pleiotropic effects of spastin on neurite growth depending on expression levels. J. Neurochem. 108, 1277–1288.
Roll-Mecak, A., Vale, R.D., 2008. Structural basis of microtubule severing by the hereditary spastic paraplegia protein spastin. Nature 451, 363–367.
Rose, K.M., 2021. When in need of an ESCRT: the nature of virus assembly sites suggests mechanistic parallels between nuclear virus egress and retroviral budding. Viruses 13, 1138.
Rose, K.M., Hirsch, V.M., Bouamr, F., 2020. Budding of a retrovirus: some assemblies required. Viruses 12, 1188.
Sakoe, K., Shioda, N., Matsuura, T., 2021. A newly identified NES sequence present in spastin regulates its subcellular localization and microtubule severing activity. Biochim. Biophys. Acta Mol. Cell Res. 1868, 118862.
Sherer, N.M., Lehmann, M.J., Jimenez-Soto, L.F., Ingmundson, A., Horner, S.M., Cicchetti, G., Allen, P.G., Pypaert, M., Cunningham, J.M., Mothes, W., 2003. Visualization of retroviral replication in living cells reveals budding into multivesicular bodies. Traffic 4, 785–801.
Solowska, J.M., Baas, P.W., 2015. Hereditary spastic paraplegia SPG4: what is known and not known about the disease. Brain 138, 2471–2484.
Solowska, J.M., Rao, A.N., Baas, P.W., 2017. Truncating mutations of SPAST associated with hereditary spastic paraplegia indicate greater accumulation and toxicity of the M1 isoform of spastin. Mol. Biol. Cell 28, 1728–1737.
Strack, B., Calistri, A., Craig, S., Popova, E., Gottlinger, H.G., 2003. AIP1/ALIX is a binding partner for HIV-1 p6 and EIAV p9 functioning in virus budding. Cell 114, 689–699.
Streck, N.T., Carmichael, J., Buchkovich, N.J., 2018. Nonenvelopment role for the ESCRT-III complex during human cytomegalovirus infection. J. Virol. 92, e02096–17.
Su, Y., Qiao, W., Guo, T., Tan, J., Li, Z., Chen, Y., Li, X., Li, Y., Zhou, J., Chen, Q., 2010. Microtubule-dependent retrograde transport of bovine immunodeficiency virus. Cell Microbiol. 12, 1098–1107.
Tavares, L.A., Januario, Y.C., daSilva, L.L.P., 2021. HIV-1 hijacking of host ATPases and GTPases that control protein trafficking. Front. Cell Dev. Biol. 9, 622610.
Tian, X., Hong, B., Zhu, X., Kong, D., Wen, Y., Wu, Y., Ma, L., Ying, T., 2022. Characterization of human IgM and IgG repertoires in individuals with chronic HIV-1 infection. Virol. Sin. 37, 370–379.
Vajente, N., Norante, R., Redolfi, N., Daga, A., Pizzo, P., Pendin, D., 2019. Microtubules stabilization by mutant spastin affects ER morphology and Ca(2+) handling. Front. Physiol. 10, 1544.
Wilen, C.B., Tilton, J.C., Doms, R.W., 2012. HIV: cell binding and entry. Cold Spring Harb Perspect. Med. 2, a006866.
Yang, D., Rismanchi, N., Renvoise, B., Lippincott-Schwartz, J., Blackstone, C., Hurley, J.H., 2008. Structural basis for midbody targeting of spastin by the ESCRT-III protein CHMP1B. Nat. Struct. Mol. Biol. 15, 1278–1286.
Yang, Q., Zhang, Q., Zhang, X., You, L., Wang, W., Liu, W., Han, Y., Ma, C., Xu, W., Chen, J., Yang, H., Wan, P., Zhou, Y., Liu, Y., Wu, K., Yang, Z., Wu, J., 2019. HoxA10 facilitates SHP-1-Catalyzed dephosphorylation of p38 MAPK/STAT3 to repress hepatitis B virus replication by a feedback regulatory mechanism. J. Virol. 93, e01607–e01618.
Yang, X., Lennard, K.R., He, C., Walker, M.C., Ball, A.T., Doigneaux, C., Tavassoli, A., van der Donk, W.A., 2018. A lanthipeptide library used to identify a protein-protein interaction inhibitor. Nat. Chem. Biol. 14, 375–380.
Yoder, A., Yu, D., Dong, L., Iyer, S.R., Xu, X., Kelly, J., Liu, J., Wang, W., Vorster, P.J., Agulto, L., Stephany, D.A., Cooper, J.N., Marsh, J.W., Wu, Y., 2008. HIV envelope-CXCR4 signaling activates cofilin to overcome cortical actin restriction in resting CD4 T cells. Cell 134, 782–792.
Yu, D., Wang, W., Yoder, A., Spear, M., Wu, Y., 2009. The HIV envelope but not VSV glycoprotein is capable of mediating HIV latent infection of resting CD4 T cells. PLoS Pathog. 5, e1000633.
Zhang, Z., Yuan, S., Xu, S., Guo, D., Chen, L., Hou, W., Wang, M., 2021. Suppression of HIV-1 integration by targeting HIV-1 integrase for degradation with A chimeric ubiquitin ligase. Virol. Sin. 36, 424–437.